J Herbmed Pharmacol. 2026; 15(1): 95-108.

http://www.herbmedpharmacol.com doi: 10.34172/jhp.2026.53352

Journal of Herbmed Pharmacology

Antidiabetic effect of *Saurauia bracteosa* through GSK-3β inhibition: Insights from phytochemical analysis, molecular docking, and glucose uptake in L6 cells

Marianne Marianne[1*], Poppy Anjelisa Zaitun Hasibuan[1*], Yuandani[1], Kamal Rullah[2], Md. Nazim Uddin[3], Yoon A Jeon[4], Young Jae Lee[4]

[1]Department of Pharmacology and Clinical/Community Pharmacy, Faculty of Pharmacy, Universitas Sumatera Utara, Medan 20155, Indonesia
[2]Department of Pharmaceutical Chemistry, Kulliyah of Pharmacy, International Islamic University Malaysia, Kuantan 25200, Pahang, Malaysia
[3]Institute of Food Science and Technology, Bangladesh Council of Scientific and Industrial Research, Dhaka 1205, Bangladesh
[4]College of Veterinary Medicine, Jeju National University, Jeju 63243, Republic of Korea

ARTICLE INFO

Article Type:
Original Article

Article History:
Received: 22 Aug. 2025
Revised: 20 Nov. 2025
Accepted: 21 Nov. 2025
epublished: 1 Jan. 2026

Keywords:
Diabetes mellitus
Glycogen synthase kinase 3
Plant extracts
Flavonoids
Triterpenes

ABSTRACT

Introduction: *Saurauia bracteosa* is a medicinal plant traditionally used by the Batak Toba and Karo ethnic groups of North Sumatra, Indonesia, to manage type 2 diabetes mellitus (T2DM). However, the precise molecular mechanisms responsible for its antidiabetic effect remain unclear. Thus, the purpose of this study was to investigate the mechanisms of action of *S. bracteosa* leaf extract and assess its potential in treating type 2 diabetes.

Methods: Phytochemical profiling was conducted using LC-MS/MS and GC-MS. Key active compounds, including ursolic acid and quercetin, were quantified by UPLC, and their effects on glucose uptake in L6 skeletal muscle cells were evaluated. To learn more about possible molecular pathways, network pharmacology and molecular docking were used.

Results: The extract was found to contain triterpenoids and flavonoids such as ursolic acid and quercetin, which significantly enhanced glucose uptake in L6 cells with effects comparable to insulin ($P>0.05$). Network pharmacology identified multiple gene targets, with pathway enrichment analysis highlighting glycogen synthase kinase-3 beta (GSK3β) as a central protein. Molecular docking confirmed the strong binding affinity of quercetin to GSK3β, supporting its potential role in modulating insulin signaling.

Conclusion: These results suggest that GSK3β regulation and enhanced glucose absorption in skeletal muscle cells may be involved in the antidiabetic action of *S. bracteosa*. This provides a scientific basis for its traditional use and highlights its potential for further development as a natural therapeutic option for diabetes.

Implication for health policy/practice/research/medical education:
The results of this research substantiate the traditional use of *S. bracteosa* leaves in managing diabetes by promoting glucose uptake through multiple bioactive compounds that act on diverse molecular targets. These results may contribute to the development of standardized herbal formulations and inform health policy regarding the regulation of traditional medicines. For clinical practice, the study provides a scientific rationale for further preclinical and clinical evaluation of *S. bracteosa*. For research, it highlights the importance of integrating phytochemical profiling, functional assays, and in silico approaches in natural product studies. In medical education, this work can serve as an example of translational ethnopharmacology, bridging traditional knowledge with modern pharmacological validation.

Please cite this paper as: Marianne M, Hasibuan PAZ, Yuandani, Rullah K, Uddin Md N, Jeon YA, et al. Antidiabetic effect of *Saurauia bracteosa* through GSK-3β inhibition: Insights from phytochemical analysis, molecular docking, and glucose uptake in L6 cells. J Herbmed Pharmacol. 2026;15(1):95-108. doi: 10.34172/jhp.2026.53352.

Introduction

One of the health issues with the fastest global growth is diabetes (1). Around 200 million people globally had diabetes in 1990, but by 2022, that figure rose to 830 million, according to the World Health Organization (WHO) (2). In addition, according to the International

***Corresponding authors**: Marianne Marianne, Email: marianne80@usu.ac.id; Poppy Anjelisa Zaitun Hasibuan, Email: poppyanjelisa@usu.ac.id

Diabetes Federation's (IDF's) Diabetes Atlas, 589 million adults aged 20-79 had diabetes in 2024; by 2050, this number is anticipated to rise to 853 million (1).

Several medications are currently available to manage diabetes mellitus; however, therapeutic failure rates remain high, and various adverse effects often limit their use in certain patients. Sulfonylureas and meglitinides can cause hypoglycemia and weight gain (3). Metformin is associated with gastrointestinal disturbances and, with long-term use, a risk of vitamin B12 and folate deficiency (4). Similar issues occur with several other drug classes. Based on these limitations, the search for new agents must continue to develop therapies with better efficacy and fewer adverse effects. Accordingly, increasing attention has been directed toward natural products, particularly medicinal plants, which offer a valuable source of bioactive compounds that may provide safer and more effective antidiabetic agents.

Saurauia bracteosa is an endemic plant in North Sumatra, Indonesia, that has been traditionally used as an antidiabetic remedy by the Batak Toba and Karo people (5,6). Scientific research on the antidiabetic activity of *S. bracteosa* leaves remains limited. Previous *in vivo* investigations have primarily focused on the n-hexane and ethyl acetate fractions, demonstrating that both fractions exhibit notable hypoglycemic activity in alloxan-induced diabetic rats, although their underlying mechanisms, particularly in skeletal muscle tissue, remain unexplored (7).

Actinidia chinensis, belonging to the same botanical family, has demonstrated the ability to restore phosphoinositide 3-kinase/protein kinase B (PI3K/Akt) signaling and encourage glucose transporter 4 (GLUT4) translocation in insulin-resistant circumstances, enhancing glucose absorption in L6 skeletal muscle cells. Given this phylogenetic relationship, *S. bracteosa* is hypothesized to have potential antidiabetic properties by promoting glucose uptake (8).

Skeletal muscle plays a crucial role in regulating insulin sensitivity in type 2 diabetes, as it is the primary tissue responsible for insulin-dependent glucose absorption (9). Multiple regulatory proteins in skeletal muscle participate in insulin signaling and have emerged as therapeutic targets for type 2 diabetes mellitus (T2DM), such as glycogen synthase kinase (GSK) (10,11). Therefore, the objective of the present research is to provide a thorough assessment of the antidiabetic properties of *S. bracteosa* by employing a combination of analytical and computational methods namely, phytochemical analysis using gas chromatography–mass spectrometry (GC–MS) and liquid chromatography–tandem mass spectrometry (LC–MS/MS), cell-based glucose uptake assays, and computational evaluations, including molecular docking and network pharmacology to elucidate its possible modes of action (12,13).

Materials and Methods

Chemicals

Anhydrous aluminum chloride, gallic acid, quercetin, 2,2-diphenyl-1-picrylhydrazyl (DPPH), ursolic acid, Folin–Ciocalteu reagent, and bovine serum albumin were procured from Sigma-Aldrich (St. Louis, MO, USA). Sodium carbonate, ascorbic acid, human recombinant insulin, and methanol were obtained from Merck KGaA (Darmstadt, Germany). Horse serum, fetal bovine serum (FBS), penicillin–streptomycin (Pen–Strep), TrypLE™ Express, and Dulbecco's Modified Eagle's Medium (DMEM; containing 4.5 g/L D-glucose, L-glutamine, and 110 mg/L sodium pyruvate) were supplied by Gibco, Thermo Fisher Scientific (Waltham, MA, USA). MTT reagent (3-(4,5-dimethylthiazol-2-yl)-2,5-diphenyltetrazolium bromide) was purchased from Biosesang (Seongnam, South Korea), while metformin was sourced from PT Hexpharm Jaya Laboratories (Bekasi, Indonesia). The L6 rat skeletal muscle cell line was acquired from the American Type Culture Collection (ATCC) or the Korean Cell Line Bank (KCLB No. 21458). Ethanol 98% was provided from Smartlab (Tangerang, Indonesia). All solvents used for chromatographic procedures were of analytical or HPLC grade, whereas other laboratory reagents met the standards of pro-analysis quality.

Saurauia bracteosa leaves collection and determination

Leaves of *S. bracteosa* were collected from Pangaribuan, North Tapanuli Regency, North Sumatra, Indonesia (2° 0′ 40.54″ N; 99° 9′ 57.96″ E; approximately 1,199 m above sea level). The plant material was taxonomically identified and authenticated at the Herbarium Bogoriense, National Research and Innovation Agency (BRIN), Cibinong, West Java, Indonesia. The samples included dried leaves, stems, flowers, fruits, and roots. The results, dated April 8, 2022 (B-964/IV/DI.05.07/4/2022), verified that the sample was *Saurauia bracteosa* DC., which was a member of the Actinidiaceae family.

Extraction

Saurauia bracteosa leaves weighing 6.5 kg were dried in a modified drying cabinet at a temperature of 40 °C until all leaves were dry, with water content below 10% (1.77 kg). *S. bracteosa* leaves were extracted with ethanol by maceration, following the Indonesian Herbal Pharmacopoeia (2nd edition) with slight modifications. In brief, one portion of the dried, powdered leaves was macerated with ten times the volume of solvent. The mixture was kept for 6 hours with intermittent stirring, and then left undisturbed for an additional 18 hours to complete the extraction process. The macerate was separated by filtration. Extraction was repeated with the same solvent using a volume equal to one-half of that employed in the first extraction. The procedure was reiterated with fresh solvent until the filtrate became colorless and left no residue upon drying.

The filtrates were merged and concentrated under vacuum through rotary evaporation to yield a semi-solid extract (14). A total yield of 162.84 g of extract was obtained from 1.77 kg of powdered leaves.

Phytochemical screening

A preliminary phytochemical examination of the *S. bracteosa* extract was subsequently carried out. Alkaloids, flavonoids, glycosides, saponins, tannins, steroids, and triterpenoids are examples of secondary metabolites. The procedure followed established protocols as described in previous studies (15-17).

Total phenolic content (TPC)

The Folin–Ciocalteu method was used to calculate the extract's TPC. In short, 10 µL of Folin-Ciocalteu reagent was combined with 100 µL of extract, and the mixture was incubated for 3 min. After that, 70 µL of distilled water and 20 µL of 7% Na_2CO_3 were added, and the mixture was incubated for one hour at 25 °C. A microplate reader was used to measure absorbance at 720 nm (Sunrise, Tecan, Switzerland). Results were expressed as µg gallic acid equivalents (GAE) per mg extract based on a gallic acid calibration curve (0–50 µg/mL) (18).

Total flavonoid content (TFC)

The TFC was analyzed using the aluminum chloride colorimetric method. Briefly, 100 µL of extract (1 mg/mL) was mixed with 100 µL of 2% $AlCl_3$ solution in ethanol and incubated for 15 minutes at 25 °C. Absorbance was measured at 420 nm utilizing a microplate reader (Sunrise, Tecan, Switzerland). Quantification was performed using a quercetin standard curve (0–25 µg/mL), and results were reported as µg quercetin equivalents (QE) per mg of extract (18).

Antioxidant activity (DPPH)

The antioxidant capacity was assessed utilizing the DPPH test. A 16 µg/mL DPPH solution in methanol was mixed with extract samples (20–50 µg/mL) and ascorbic acid standards (2–5 µg/mL). Following a 10-minute incubation in darkness at 25 °C, absorbance was measured at 516 nm utilizing a UV–Vis spectrophotometer (Thermo Fisher Scientific G10s, China).

Radical scavenging activity was calculated using the following formula:

Radical scavenging activity (%) = [(A_control – A_sample)/A_control] × 100.

"A_control" is the absorbance of the DPPH solution without the sample, and "A_sample" is the absorbance in the presence of the extract. IC_{50} values were calculated from the linear regression equation (y = ax + b), in which a represents the slope and b represents the intercept (19).

Liquid chromatography-tandem mass spectrometry (LC-MS/MS) analysis

An extract of *S. bracteosa* (1 mg) was solubilized in 10 µL of methanol and subjected to LC-MS/MS analysis utilizing a Waters ACQUITY UPLC I-Class system in conjunction with a Xevo G2-XS QTOF mass spectrometer (Waters Corporation, Manchester, UK). Separation was accomplished on an ACQUITY UPLC BEH C18 column utilizing a water–acetonitrile mobile phase with 0.1% formic acid under gradient elution conditions. Data were acquired in positive electrospray ionization (ESI) mode across m/z range of 100–1200, with specific instrument settings provided in Supplementary file 1 (S1).

Gas chromatography–mass spectrometry (GC–MS) analysis

The chemical components of *S. bracteosa* extract were analyzed using a GC–MS apparatus (QP2010 SE, Shimadzu, Kyoto, Japan) equipped with a Rtx-5MS capillary column. The analytical procedure was performed according to established GC–MS methodology, with specific operating parameters detailed in Supplementary file 1 (S2). Identification of volatile components was achieved by matching the acquired mass spectra with those in the reference database, and only compounds exhibiting similarity scores above 90% were considered reliable.

UPLC analysis of ursolic acid and quercetin

Standard solutions (100 ppm) of ursolic acid and quercetin were analyzed using an ACQUITY UPLC H-Class system with a PDA detector and an Xevo™ TQ-D mass spectrometer (Waters, USA). Separation was performed on a BEH C18 column (2.1 × 100 mm, 1.7 µm) at 40 °C. Ursolic acid was eluted with water–acetonitrile (30:70, v/v), while quercetin was separated using a water/acetonitrile gradient containing 0.1 % formic acid. Detection was carried out at compound-specific wavelengths under optimized negative ESI conditions. The method demonstrated good linearity (R^2 > 0.99), precision (RSD ≤ 15%), and sensitivity. Extracts (1,000 ppm) were quantified using the same calibration models. Detailed instrument parameters are provided in Supplementary file 1 (S3) (20,21).

L6 culture and cytotoxicity assay

L6 rat skeletal muscle cells were cultured in Dulbecco's Modified Eagle's Medium (DMEM) containing 4.5 g/L D-glucose, supplemented with 10% fetal bovine serum (FBS) and 1% penicillin–streptomycin. The cells were maintained at 37 °C in a humidified incubator with 5% CO_2.

The cytotoxic effects of *S. bracteosa* extract, quercetin, ursolic acid, insulin, and metformin (used as reference compounds) were assessed using the MTT

[3-(4,5-dimethylthiazol-2-yl)-2,5-diphenyl tetrazolium bromide] assay. Cell viability was calculated using the following equation (22):

$$\text{Viability}(\%) = \frac{\text{Sample absorbance}}{\text{Control absorbance}} \times 100$$

L6 glucose uptake assay

L6 myoblasts (2×10^5 cells/well) were seeded in 24-well plates and grown in DMEM for 48 hours until ~70 % confluence. Cells were then serum-starved in low-glucose DMEM (1 g/L) containing 1% Pen–Strep for 4 hours, followed by treatment with 495 µL of serum-starved low-glucose (SSL) medium and 5 µL of the test sample per well. *S. bracteosa* extract, quercetin, ursolic acid, insulin, and metformin were dissolved in DMSO or distilled water according to solubility and prepared at the desired concentrations: extract (100, 200 µg/mL), quercetin (10, 50 µM), ursolic acid (5, 10 µM), insulin (100 nM), and metformin (40 µM).

To determine baseline glucose (T_0), 10 µL of medium from each well was mixed with 190 µL of PAP-SL reagent (containing 4-aminophenazone, phenol, peroxidase, and glucose oxidase) in a 96-well plate. After 15 minutes of incubation at room temperature, the absorbance was measured at 492 nm. Glucose concentrations were determined from a standard curve (0.07–4.5 mg/mL). Glucose levels in the media were assessed at 1, 2, 3, 4, 5, 6, and 16 hours post-treatment. The amount of glucose absorbed by the cells was determined by subtracting the absorbance of the treated samples from the control, and converting the values into glucose concentration using the regression equation (23,24).

Protein target analysis

Potential molecular targets of *S. bracteosa* phytochemicals were predicted through two complementary ligand-based tools: SwissTargetPrediction and SuperPred 3.0. These web-based platforms are recognized and validated for accurately identifying possible protein targets of natural compounds (25,26).

The canonical simplified molecular input line entry system (SMILES) of each secondary metabolite, obtained from the PubChem database, was used as input for target prediction. The SwissTargetPrediction platform integrates both 2D and 3D similarity analyses with reference ligands to predict potential protein targets, whereas SuperPred utilizes machine learning algorithms based on chemical similarity to identify targets associated with approved drugs. Only predicted targets with probability scores above the recommended thresholds were retained, and the intersecting proteins predicted by both platforms were selected for further analyses. This dual approach increases reliability and reduces the likelihood of false positives, as previously demonstrated in natural product research (26).

Protein–protein interaction (PPI)

Proteins from the Venn intersection were analyzed using the STRING database (v11.0) to construct a PPI network. The resulting data (.tsv) were processed in Cytoscape 3.9.1 with CytoHubba to identify hub proteins based on topological parameters (degree, betweenness, and proximity centrality).

Functional annotation

Proteins from the PPI network were subjected to gene ontology (GO) and Kyoto Encyclopedia of Genes and Genomes (KEGG) enrichment using the database for annotation, visualization, and integrated discovery (DAVID) database (v6.8) (27). Terms with a false discovery rate (FDR) < 0.05 were considered significant for further interpretation.

Molecular docking

The 3D structure of GSK3β (PDB ID: 1Q41) was obtained from the Research Collaboratory for Structural Bioinformatics (RCSB) Protein Data Bank (PDB), and *S. bracteosa* metabolites were retrieved from PubChem. Protein and ligand preparation were done in PyMOL 2.5.2, followed by docking in AutoDock Vina (grid center: X = 39.439, Y = 6.199, Z = 36.086; size: 40 × 40 × 40 Å; exhaustiveness = 10/32). Docking interactions were visualized using Discovery Studio 2019.

Statistical analysis

GraphPad Prism 9 (GraphPad Software, USA) was used to perform a one-way ANOVA with Tukey's post hoc test on the MTT and glucose uptake assay data. The significance level was set at $P < 0.05$, and the results were presented as mean ± SD (n = 4).

Results

Phytochemical screening

The ethanolic extract of *S. bracteosa* leaves contained a variety of secondary metabolites, including alkaloids, glycosides, flavonoids, saponins, tannins, and steroids/terpenoids.

Total phenolic, total flavonoid, and antioxidant in *Saurauia bracteosa* leaf extract

The *S. bracteosa* extract exhibited a total phenolic content of 76.19 ± 2.05 µg GAE/mg extract, a total flavonoid content of 25.54 ± 0.80 µg QE/mg extract, and an antioxidant activity (IC_{50}) value of 48.26 ± 0.12 µg/mL, respectively.

LC-MS/MS analysis

The LC–MS/MS analysis revealed that the ethanolic extract of *S. bracteosa* contained compounds belonging primarily to the terpenoid, flavonoid, and steroid classes. Within the terpenoid group, the identified constituents

included 27-O-(Z)-coumaroyl-ursolic acid, 3β-O-trans-p-caffeoyl alphitolic acid, ursolic acid, oleanolic acid, corosolic acid, maslinic acid, and β-amyrin. Stigmasterol and β-sitosterol were found in the steroid fraction, but quercetin and quercetin-3-O-α-L-arabinopyranoside made up the majority of the flavonoid fraction (Table 1).

GC-MS analysis

The ethanol extract of *S. bracteosa* contained 33 chemicals, as determined by GC-MS analysis, as shown in Supplementary file 1 (S4). These belonged to diverse chemical classes, including hydrocarbons, fatty acids and esters, terpenoid alcohols, sterols, triterpenoids, and

Table 1. Component analysis of *Saurauia bracteosa* extract via liquid chromatography-tandem mass spectrometry

No.	Compound name	Molecular formula	m/z	Adducts	Neutral mass (Da)	Retention time (min)	Chemical structure
1	27-O-(Z)-Coumaroyl-ursolic acid (terpenoid)	$C_{39}H_{54}O_6$	641.38	+Na	618.39	8.79	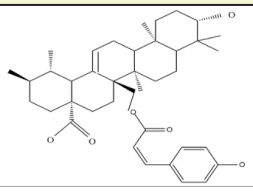
2	3β-O-trans-p-Caffeoyl alphitolic acid (terpenoid)	$C_{39}H_{54}O_7$	657.38	+Na, +H	634.39	7.55	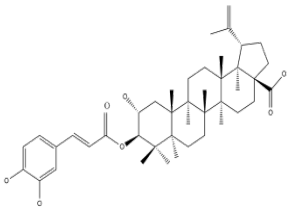
3	Quercetin (flavonoid)	$C_{15}H_{10}O_7$	303.05	+H	302.04	3.53	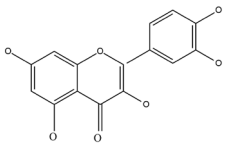
4	Quercetin-3-O-α-L-arabinopyranoside I (flavonoid)	$C_{20}H_{18}O_{11}$	435.09	+H, +Na	434.08	3.44	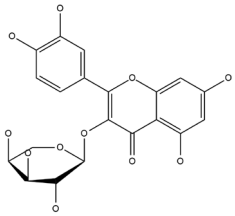
5	Ursolic acid (terpenoid)	$C_{30}H_{48}O_3$	457.37	+H	456.36	7.26	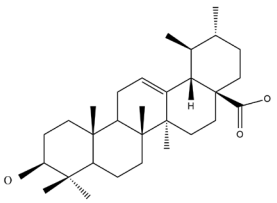
6	Oleanolic acid (terpenoid)	$C_{30}H_{48}O_3$	457.37	+H	456.36	7.26	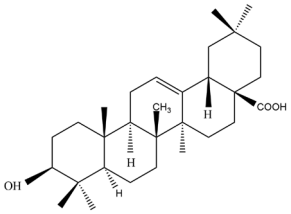
7	Corosolic acid (terpenoid)	$C_{30}H_{48}O_4$	473.36	+H	472.70	9.16	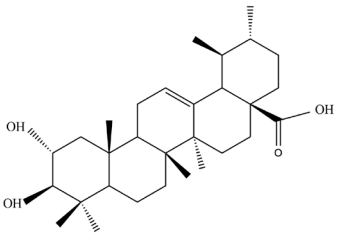

Table 1. Continued

No.	Compound name	Molecular formula	m/z	Adducts	Neutral mass (Da)	Retention time (min)	Chemical structure
8	Maslinic acid (terpenoid)	$C_{30}H_{48}O_4$	473.36	+H	472.70	9.16	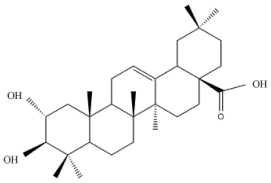
9	β-amyrin (terpenoid)	$C_{30}H_{50}O$	427.39	+H	426.72	8.84	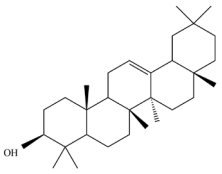
10	Stigmasterol (steroid)	$C_{29}H_{48}O$	413.38	+H	412.69	10.00	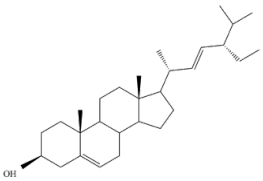
11	β-sitosterol (steroid)	$C_{29}H_{50}O$	415.39	+H	414.71	10.10	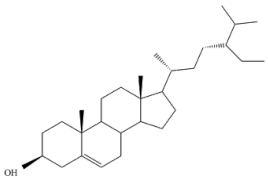

Abbreviations: m/z: mass-to-charge ratio.

tocopherols (vitamin E derivatives), as well as minor lactones and benzofuran derivatives. The most abundant constituents were phytol (16.2%), γ-sitosterol (13.5%), and stigmasterol (5.9%). This chemical diversity suggests that the extract contains multiple bioactive metabolites with potential antioxidant and antidiabetic activities.

Ursolic acid and quercetin content

Chromatographic analysis of *S. bracteosa* leaf extract was conducted alongside standard compounds to confirm the presence of ursolic acid and quercetin (Figure 1). Ursolic acid was eluted at 4.3 minutes and quercetin at 4.8 minutes (Table 2). Ursolic acid displayed a substantially greater area under the curve (AUC = 252,388) compared with quercetin (AUC = 1,420), suggesting that ursolic acid was present in considerably higher amounts within the extract. The concentration of ursolic acid was determined to be 23.9 ppm, with a relative content of 2.39%. In contrast, quercetin was present at a concentration of 0.9 ppm, with a relative content of 0.09%. These results suggest that ursolic acid is the predominant compound in the extract.

The linearity and sensitivity parameters of ursolic acid and quercetin were determined using calibration curves generated through UPLC analysis. Both compounds demonstrated excellent linearity, with R^2 of 0.9999 for ursolic acid and 0.9982 for quercetin, indicating linear correlations between concentration and detector response (Table 3). Furthermore, the UPLC method demonstrated excellent analytical sensitivity, as reflected by its low detection and quantification limits. The limit of detection (LOD) values were 2.213 mg/L for ursolic acid and 0.020 mg/L for quercetin, representing the minimum concentrations that could be reliably detected. The limit of quantification (LOQ) values were 6.705 mg/L for ursolic acid and 0.062 mg/L for quercetin, representing the minimum concentrations that could be quantified with satisfactory precision and accuracy.

Cytotoxicity in L6 cells

Cell viability was evaluated after exposing L6 cells to varying concentrations of the *S. bracteosa* extract, quercetin, ursolic acid, insulin, and metformin (Figure 2). Based on the cytotoxicity outcomes, non-toxic concentrations of the extract and standard compounds were selected for the subsequent glucose uptake experiments. The working concentrations applied in the assay were: insulin (100 nM), *S. bracteosa* extract (100 and 200 µg/mL), ursolic acid (5 and 10 µM), quercetin (10 and 50 µM), and metformin (40 µM). Doses were selected based on viability data, which showed no significant reduction in cell survival relative to the untreated control ($P > 0.05$).

Glucose uptake in L6 cells

The calibration curve for glucose showed excellent

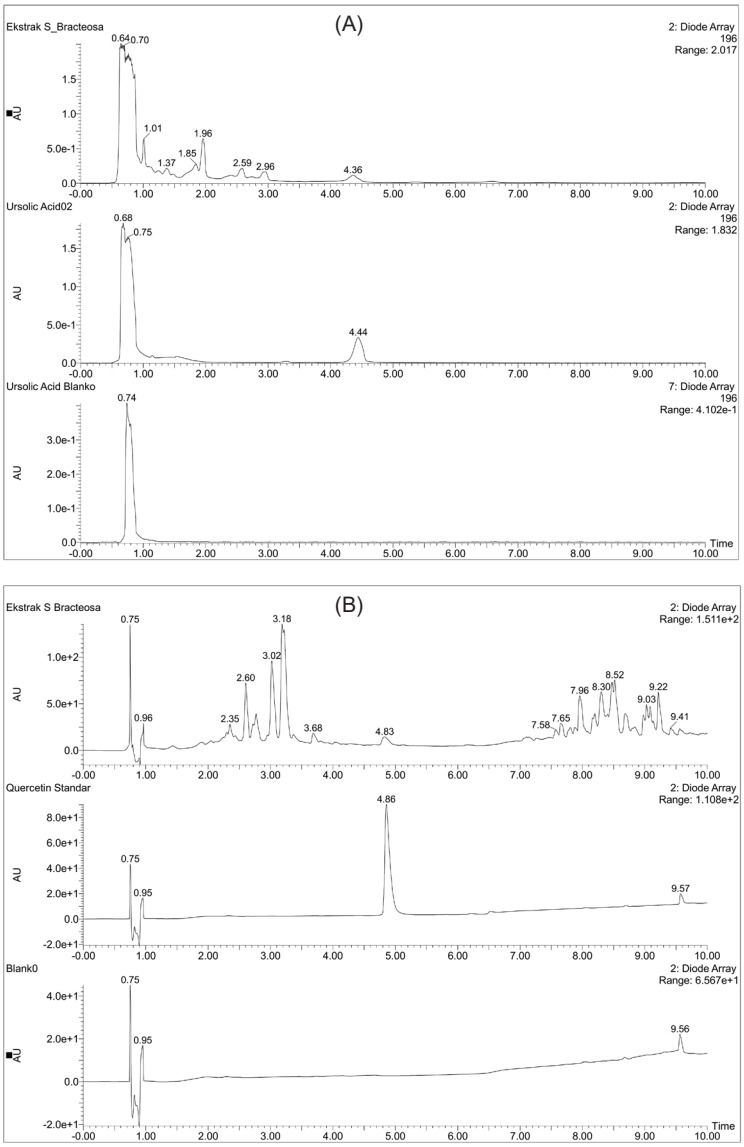

Figure 1. Representative ultra-performance liquid chromatography (UPLC) chromatograms of *Saurauia bracteosa* leaf extract, standard, and blank. (A) ursolic acid and (B) quercetin.

linearity (y = 0.7172x + 0.0948, R^2 = 0.999), confirming the accuracy of concentration determinations. Glucose uptake in L6 cells was then assessed at 0, 1, 2, 3, 4, 5, 6, and 16 hours to monitor the translocation of glucose from the extracellular medium into the cells. No noticeable variation in glucose uptake was detected between the treated groups and the normal control during the initial incubation period (0–4 hours) (Figure 3A). A distinct elevation in glucose uptake became apparent after 5–6 hours of treatment, indicating enhanced glucose utilization in the test groups. By the 16-hour mark, values for glucose uptake had stabilized and were now comparable to those of the control. The greatest stimulatory response occurred at the 5-hour time point, where all tested samples, including the ethanolic extract of *S. bracteosa* leaves, generated a notable increase in glucose absorption compared to the untreated control group ($P < 0.05$) (Figure 3B). At this point, the effects of insulin (100 nM) were comparable to those of

Table 2. Quantifying ursolic acid and quercetin in Saurauia bracteosa leaf extract using ultra-performance liquid chromatography (UPLC)

Compound	Extract weight (mg)	Retention time (min)	AUC	Concentration (ppm)	Dilution factor	Volume (mL)	Content (mg/g extract)	Relative content (%)
Ursolic acid	10	4.3	252,388	23.9	10	1	23.9	2.39
Quercetin	10	4.8	1,420	0.9	10	1	0.9	0.09

Abbreviation: AUC, area under the curve.

Table 3. Linearity and detection sensitivity of the ultra-performance liquid chromatography (UPLC) method used for quantifying ursolic acid and quercetin

Compound	Linearity			Sensitivity	
	Calibration	R^2	Linear range (mg/L)	LoD (mg/L)	LoQ (mg/L)
Ursolic acid	y = 10635x – 1811	0.9999	7.81 – 250.00	2.213	6.705
Quercetin	y = 3469.1x + 217.73	0.9982	0.24 – 7.84	0.020	0.062

Abbreviations: LoD, Limits of detection; LoQ, Limits of quantification.

ursolic acid (5 µM) and quercetin (50 µM). Notably, the ethanol extract of *S. bracteosa*, ursolic acid, and quercetin did not demonstrate a dose-dependent increase in glucose uptake, indicating that their effects were consistent across different concentrations.

Furthermore, the extract and individual compounds—quercetin, ursolic acid, and metformin—enhanced glucose uptake, with the most pronounced effect observed 5 hours after treatment.

Protein-protein interaction

SwissTargetPrediction identified 179 target proteins, whereas SuperPred identified 208 target proteins from the secondary metabolites shown in Supplementary file 1 (S5). The obtained proteins were classified into various target classes, including G protein-coupled receptor, oxidoreductase, kinase, cytochrome P450, protease, lyase, primary active transporter, unclassified protein, eraser, isomerase, hydrolase, phosphatase, nuclear receptor, electrochemical transporter, other cytosolic proteins, transcription factors, membrane receptors, and secreted proteins.

The obtained data were then input into the Draw Venn Diagram website, producing 51 relationships between the protein targets of bioactive compounds and the protein targets of T2DM (Figure 4).

The PPI study was conducted using the STRING database to explore potential relationships among the predicted target proteins. This platform integrates experimental and predicted interaction data, allowing comprehensive mapping of molecular connections that reflect the functional associations and biological pathways underlying cellular processes.

The interaction relationships among all predicted target

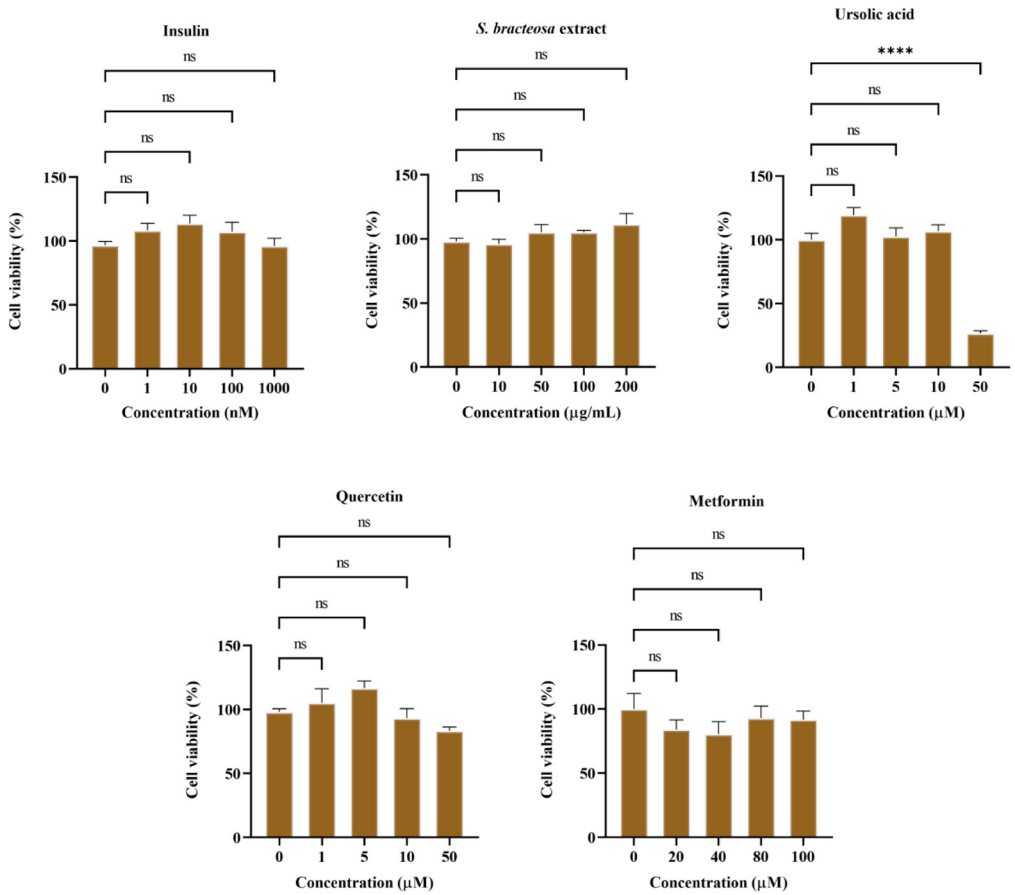

Figure 2. Cell viability of L6 cells after exposure to varying concentrations of insulin, *Saurauia bracteosa* extract, quercetin, ursolic acid, and metformin. The values (n = 4) are displayed as mean ± SD. ****$P < 0.0001$ compared to the untreated control.

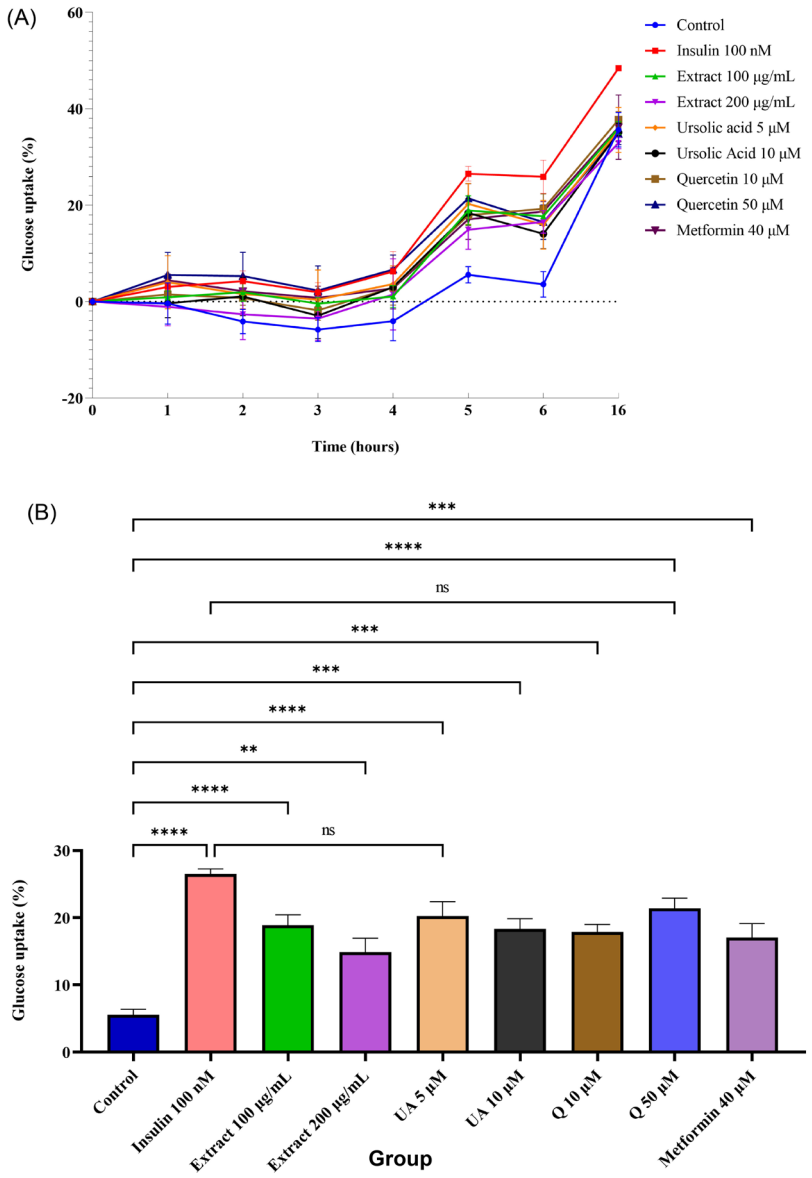

Figure 3. Effects of *Saurauia bracteosa* extract and reference compounds on glucose uptake in L6 skeletal muscle cells. **(A)** Time-dependent glucose uptake over 0-16 h; **(B)** Glucose uptake rate at the 5 h time point showing the comparative effects of each treatment. The data (n = 4) are presented as mean ± standard deviation. ****$P < 0.0001$; **$P < 0.01$; ***$P < 0.005$; ns: not significant ($P > 0.05$).

proteins were visualized in Supplementary file 1 (S6).

Functional annotation

Functional annotation assigns a biological or functional role to a protein based on experimental evidence or predictions from various data sources, thereby elucidating the functions of proteins within broader biological systems. The identified hub genes are shown in Figure 5. Enrichment analysis revealed significant associations of these proteins with biological process (BP), cellular component (CC), and molecular function (MF) categories (FDR < 0.05), as illustrated in Figure 6.

As illustrated in Figure 6, the main molecular functions identified included insulin receptor interaction, transmembrane receptor protein tyrosine kinase function, and protein tyrosine kinase activity. The BP target proteins were positive regulators of kinase activity, protein autophosphorylation, and transmembrane receptor proteins.

Molecular docking

The results of re-docking the receptor with PDB code 1Q41 against the native ligand showed an RMSD value of 0.401 Å for the GSK3β. Based on this value, the receptor met the requirements for an RMSD value of ≤ 2 Å based on previous research. Thus, obtaining an appropriate RMSD facilitates analysis at the molecular docking testing stage using AutoDock Vina software.

Table 4 shows that quercetin exhibited strong binding to GSK3β (−9.1 ± 0.0 kcal/mol), comparable to the native

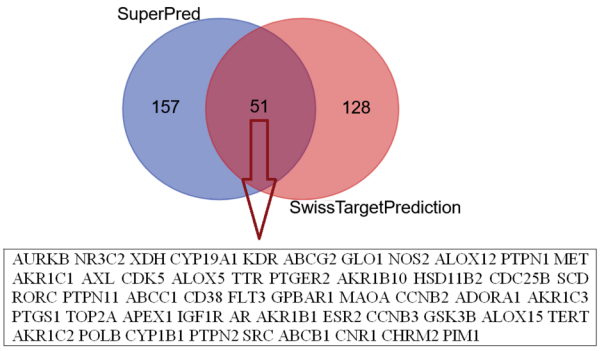

Figure 4. Venn diagram showing 51 common target genes interacting with *Saurauia bracteosa* active compounds.

ligand (−9.8 ± 0.1 kcal/mol), and stronger than pioglitazone (−7.1 ± 0.1 kcal/mol) or metformin (−4.9 ± 0.1 kcal/mol). Quercetin formed hydrogen bonds with VAL135 and hydrophobic contacts with VAL110, ALA83, LEU132, and VAL70, overlapping with native ligand interactions. Detailed docking score and residue interactions are provided in Supplementary file 1 (S7 and S8).

Discussion

Approximately 80% of insulin-mediated glucose uptake occurs in skeletal muscle, making it a primary site for maintaining glucose homeostasis and a major therapeutic target in T2DM (30). Activation of the insulin signaling cascade via the IRS–PI3K–Akt axis facilitates the migration of GLUT4 to the cell surface, while suppressing glycogen synthase kinase-3β (GSK3β), a key inhibitor of glycogen formation. Disturbance of this signaling network results in reduced glucose uptake and the onset of insulin resistance (29,30). This overview serves as the foundation for the subsequent discussion on GSK3β and GLUT4.

In this study, the chemical profiling of *S. bracteosa* identified diverse secondary metabolites, among which quercetin (a flavonoid) and ursolic acid (a triterpenoid)

Figure 5. Kyoto Encyclopedia of Genes and Genomes (KEGG) pathway enrichment of the anticipated target genes implicated in the antidiabetic activity of *Saurauia bracteosa*. A threshold of false discovery rate (FDR < 0.05) was applied to identify statistically significant.

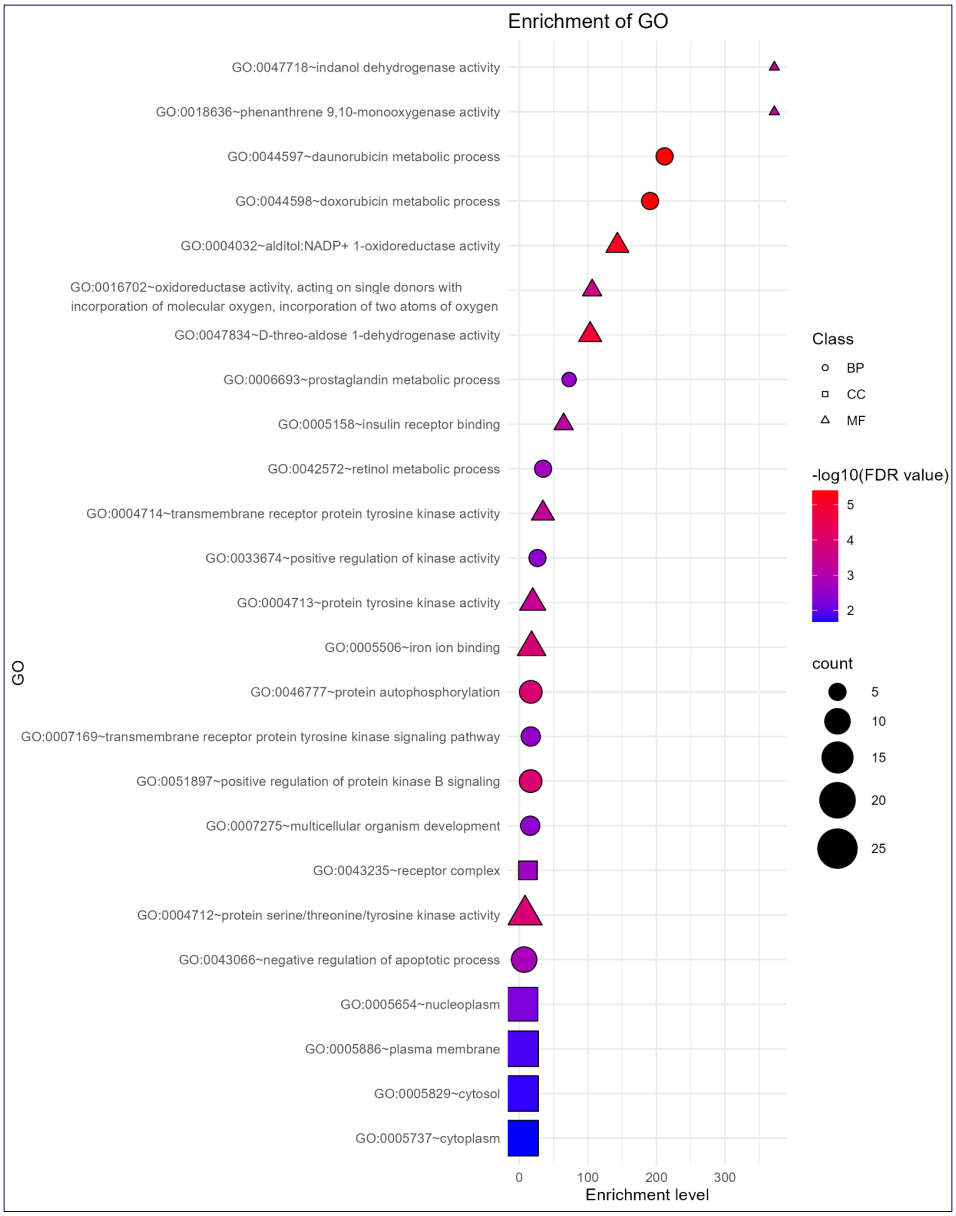

Figure 6. The top 10 enriched Gene Ontology (GO) terms for biological process (BP), cellular component (CC), and molecular function (MF) associated with the hub genes targeted by *Saurauia bracteosa* extract phytochemicals. A threshold of false discovery rate (FDR < 0.05) was applied to identify statistically significant pathways.

were quantified by UPLC as key constituents. Ursolic acid was present at higher levels (2.39%) compared with quercetin (0.09%), providing a pharmacological rationale for its contribution to activity.

Functionally, the L6 skeletal muscle cells' uptake of glucose was enhanced by the crude extract and its active ingredients. Quercetin (50 µM) and ursolic acid (5 µM) produced responses similar to insulin, indicating an insulin-mimetic effect. These results demonstrate that *S. bracteosa* exerts insulin-like activity by stimulating glucose transport in L6 cells, in agreement with the actions of its isolated compounds. The stronger response at a lower ursolic acid concentration reflects its higher proportion in the extract, implying a possible synergistic role with quercetin in enhancing glucose uptake within skeletal muscle cells. These effects provide experimental validation of the traditional claim that the plant improves glycemic control.

To further clarify the molecular basis of these effects, network pharmacology analysis revealed three key hub proteins, SRC, GSK3β, and MET, strongly linked to insulin resistance and diabetes-related signaling pathways (31-33). While literature linking SRC and MET to diabetes is relatively limited, GSK3β has been extensively implicated in impaired insulin signaling, glycogen metabolism, and glucose homeostasis. Due to its strong mechanistic relevance and robust literature support, GSK3β was selected as the primary docking target to rationalize the

Table 4. Molecular docking outcomes of *Saurauia bracteosa* constituents with GSK3β

Secondary metabolites	Average of ∑ docking score (kcal/mol) ± SD
Native ligand (Z)-1h,1'h [2,3']-Biindolylidene-3,2'-Dione-3-Oxime	-9.8 ± 0.1
Pioglitazone	-7.1 ± 0.1
Metformin	-4.9 ± 0.1
Quercetin	-9.1 ± 0.0

observed insulin-mimetic activity of the extract and its compounds.

Docking studies confirmed that quercetin exhibited strong affinity for GSK3β (–9.1 ± 0.0 kcal/mol), comparable to the native ligand (–9.8 ± 0.1 kcal/mol), with interactions at Val135 overlapping those of the native ligand. In contrast, ursolic acid showed weaker binding, suggesting that its glucose-uptake activity may proceed through complementary mechanisms rather than direct inhibition of GSK3β.

Taken together, these findings suggest that quercetin likely enhances glucose uptake through direct modulation of GSK3β, while ursolic acid may act via alternative mechanisms, potentially involving other network-identified targets, such as SRC or MET. The multi-component, multi-target profile of *S. bracteosa* extract is consistent with its ethnopharmacological use as an antidiabetic remedy, illustrating the advantage of integrating phytochemical characterization, *in vitro* assays, and *in silico* predictions.

This study has several limitations. The mechanistic insights are based on network predictions and docking simulations; direct confirmation (e.g., western blot for GSK3β or GLUT4 translocation assays) is warranted. Furthermore, this study was limited to in vitro tests; additional in vivo research is necessary to validate the safety and effectiveness of the extract.

Conclusion

In summary, the extract of *S. bracteosa* and its major compounds, ursolic acid and quercetin, markedly promote the uptake of glucose in cells of skeletal muscle. By targeting multiple proteins involved in insulin resistance, including GSK3β, SRC, and MET, the extract may exhibit synergistic actions that validate its traditional use as an antidiabetic agent. These integrated findings provide mechanistic insights and a foundation for the further development of *S. bracteosa* as a potential phytopharmaceutical for the treatment of type 2 diabetes.

Declaration of artificial intelligence (AI) use in scientific writing

The authors declare that AI–assisted technologies, including ChatGPT (OpenAI, San Francisco, CA, USA), were used solely to enhance grammar and clarity in the manuscript. All scientific content, data acquisition, analysis, and interpretation were generated and verified by the authors.

Authors' contribution

Conceptualization: All authors.
Data curation: Marianne Marianne.
Formal analysis: All authors.
Funding acquisition: Marianne Marianne, Poppy Anjelisa Zaitun Hasibuan, Yuandani, Young Jae Lee.
Investigation: Marianne Marianne.
Methodology: All authors.
Project administration: Marianne Marianne.
Resources: Marianne Marianne.
Software: Md. Nazim Uddin, Yoon A Jeon, Young Jae Lee.
Supervision: Poppy Anjelisa Zaitun Hasibuan, Yuandani, Kamal Rullah.
Validation: Poppy Anjelisa Zaitun Hasibuan, Yuandani, Kamal Rullah, Yoon A Jeon, Young Jae Lee.
Visualization: Marianne Marianne, Kamal Rullah, Md. Nazim Uddin, Yoon A Jeon, Young Jae Lee.
Writing–original draft: Marianne Marianne, Poppy Anjelisa Zaitun Hasibuan, Yuandani, Kamal Rullah.
Writing–review & editing: All authors.

Conflict of interests

The authors confirm that there are no conflicts of interest associated with this publication.

Funding

This study was supported by the Directorate of Research, Technology, and Community Service, Ministry of Education, Culture, Research, and Technology of Indonesia (Grant No. 0267/E5/Ak.04/2022, April 28 2022) and by the Talenta Research Program, Universitas Sumatera Utara (Grant No. 1705/UN5.1.R/SK/PPM/2022, July 20 2022).

Supplementary files

Supplementary file 1 contains the follwing sections:

- S1. LC-MS/MS analysis.
- S2. GC-MS analysis.
- S3. Specific instrument settings for UPLC–MS analysis of ursolic acid and quercetin.
- S4. Secondary metabolites identified in *Saurauia bracteosa* leaf extract by GC-MS.
- S5. The predicted genes were identified using SwissTargetPrediction.
- S6. Protein–protein interaction network of 51 target genes linked to *Saurauia bracteosa* compounds.
- S7. Molecular docking of *Saurauia bracteosa* compounds with GSK3β.
- S8. 2D visualization of the interacting amino acid residues with the GSK3β receptor.

References

1. International Diabetes Federation (IDF). IDF Global Clinical Practice Recommendations for Managing Type 2 Diabetes. Brussels: IDF; 2025. Available from: https://idf.org/media/uploads/2025/04/IDF_Rec_2025.pdf.
2. World Health Organization (WHO). Diabetes Fact Sheet. Geneva: WHO; 2024. Available from: https://www.who.int/news-room/fact-sheets/detail/diabetes.
3. Timmons J, Boyle J. Sulfonylureas and meglitinides. In: Fisher M, Mckay GA, Llano A, eds. Diabetes Drug Notes. John Wiley & Sons; 2022. p. 49-66. doi: 10.1002/9781119785033.ch3.
4. Mazumder A, Singh A. A review on metformin: clinical significance and side effects. Res J Pharm Technol. 2021;14(11):6179-86. doi: 10.52711/0974-360x.2021.01070.
5. Situmorang RO, Sunandar AD. Pirdot (*Saurauia bracteosa* DC) leaf processing technique for making herbal tea. IOP Conf Ser Earth Environ Sci. 2019;359(1):012004. doi: 10.1088/1755-1315/359/1/012004.
6. Pasaribu G, Budianto E, Cahyana H, Saepudin E. A review on genus *Saurauia*: chemical compounds and their biological activity. Pharmacogn J. 2020;12(3):657-66. doi: 10.5530/pj.2020.12.97.
7. Murtihapsari M, Situmeang B, Suparman AR, Parubak AS, Yogaswara R, Susilawati Y, et al. Aktivitas antidiabetes dari fraksi *Sauauria bracteosa* pada tikus dengan metode induksi aloksan. Jamb J Chem. 2022;4(1):1-9. doi: 10.34312/jambchem.v4i1.11659.
8. Kim JH, Kim JW, Kim SC, Lee YJ. Kiwifruit (*Actinidia chinensis*) extract annuls chronic insulininduced insulin resistance in l6 skeletal muscle cells. Food Science and Biotechnology. 2013;22(4):1091-6. doi: 10.1007/s10068-013-0188-4.
9. Kumar N, Kaushik NK, Park G, Choi EH, Uhm HS. Enhancement of glucose uptake in skeletal muscle L6 cells and insulin secretion in pancreatic hamster-insulinoma-transfected cells by application of non-thermal plasma jet. Appl Phys Lett. 2013;103(20):203701. doi: 10.1063/1.4828742.
10. Huang X, Liu G, Guo J, Su Z. The PI3K/AKT pathway in obesity and type 2 diabetes. Int J Biol Sci. 2018;14(11):1483-96. doi: 10.7150/ijbs.27173.
11. Petersen MC, Shulman GI. Mechanisms of insulin action and insulin resistance. Physiol Rev. 2018;98(4):2133-223. doi: 10.1152/physrev.00063.2017.
12. Baig MW, Fatima H, Akhtar N, Hussain H, Okla MK, Al-Hashimi A, et al. Anti-inflammatory potential of daturaolone from *Datura innoxia* Mill.: in silico, in vitro and in vivo studies. Pharmaceuticals (Basel). 2021;14(12):1248. doi: 10.3390/ph14121248.
13. Noor F, Tahir Ul Qamar M, Ashfaq UA, Albutti A, Alwashmi AS, Aljasir MA. Network pharmacology approach for medicinal plants: review and assessment. Pharmaceuticals (Basel). 2022;15(5):572. doi: 10.3390/ph15050572.
14. Ministry of Health Republic of Indonesia. Indonesian Herbal Pharmacopoeia. 2nd ed. Jakarta: Ministry of Health Republic of Indonesia; 2017. p. 546.
15. Farnsworth NR. Biological and phytochemical screening of plants. J Pharm Sci. 1966;55(3):225-76. doi: 10.1002/jps.2600550302.
16. Harborne AJ. Phytochemical Methods a Guide to Modern Techniques of Plant Analysis. 3rd ed. New York: Chapman & Hall; 1998. p. 198.
17. Sivanandham V. Phytochemical techniques-a review. World J Sci Res. 2015;1(2):80-91.
18. Jeon YA, Chung SW, Kim SC, Lee YJ. Comprehensive assessment of antioxidant and anti-inflammatory properties of papaya extracts. Foods. 2022;11(20):3211. doi: 10.3390/foods11203211.
19. Marianne M, Harahap U, Hasibuan PA, Thampati CM, Harefa HS. Hepatoprotective activity of the ethanol extract of *Curcuma heyneana* rhizome on isoniazid and rifampin-induced liver injury rats. J Herbmed Pharmacol. 2020;9(4):333-8. doi: 10.34172/jhp.2020.42.
20. Putra N, Garmana AN, Qomaladewi NP, Amrianto, Al Muqarrabun LM, Rosandy AR, et al. Bioactivity-guided isolation of a bioactive compound with α-glucosidase inhibitory activity from the leaves extract of *Sauropus androgynus*. Sustain Chem Pharm. 2023;31:100907. doi: 10.1016/j.scp.2022.100907.
21. Yuandani, Jantan I, Husain K. 4,5,4'-Trihydroxychalcone, 8,8'-(ethene-1,2-diyl)-dinaphtalene-1,4,5-triol and rutin from *Gynura segetum* inhibit phagocytosis, lymphocyte proliferation, cytokine release and nitric oxide production from phagocytic cells. BMC Complement Altern Med. 2017;17(1):211. doi: 10.1186/s12906-017-1726-z.
22. Edirs S, Jiang L, Xin X, Aisa HA. Anti-diabetic effect and mechanism of *Kursi Wufarikun Ziyabit* in L6 rat skeletal muscle cells. J Pharmacol Sci. 2018;137(2):212-9. doi: 10.1016/j.jphs.2018.06.011.
23. Hutapea A, Hutahaean S, Ilyas SY. Influence of pirdot leaf (*Saurauia vulcani*, Korth.) extract on the blood glucose rate and histologic description of the retina of male mice (*Mus musculus* strain DDW). Asian J Pharm Clin Res. 2018;11(11):389-92. doi: 10.22159/ajpcr.2018.v11i11.28316.
24. Salim E, Fatimah C, Fanny DY. analgetic activity of cep-cepan (*Saurauia cauliflora* DC.) leaves extract. Jurnal Natural. 2017;17(1):31-8. doi: 10.24815/jn.v17i1.6856.
25. Daina A, Michielin O, Zoete V. SwissTargetPrediction: updated data and new features for efficient prediction of protein targets of small molecules. Nucleic Acids Res. 2019;47(W1):W357-64. doi: 10.1093/nar/gkz382.
26. Gallo K, Goede A, Preissner R, Gohlke BO. SuperPred 3.0: drug classification and target prediction-a machine learning approach. Nucleic Acids Res. 2022;50(W1):W726-31. doi: 10.1093/nar/gkac297.
27. Sherman BT, Hao M, Qiu J, Jiao X, Baseler MW, Lane HC, et al. DAVID: a web server for functional enrichment analysis and functional annotation of gene lists (2021 update). Nucleic Acids Res. 2022;50(W1):W216-21. doi: 10.1093/nar/gkac194.
28. Merz KE, Thurmond DC. Role of skeletal muscle in insulin resistance and glucose uptake. Compr Physiol. 2020;10(3):785-809. doi: 10.1002/cphy.c190029.
29. van Gerwen J, Shun-Shion AS, Fazakerley DJ. Insulin signalling and GLUT4 trafficking in insulin resistance. Biochem Soc Trans. 2023;51(3):1057-69. doi: 10.1042/bst20221066.
30. Whytock KL, Goodpaster BH. Unraveling skeletal muscle insulin resistance: molecular mechanisms and the

restorative role of exercise. Circ Res. 2025;137(2):184-204. doi: 10.1161/circresaha.125.325532.
31. Ye C, Li Y, Shi J, He L, Shi X, Yang W, et al. Network pharmacology analysis revealed the mechanism and active compounds of jiao tai wan in the treatment of type 2 diabetes mellitus via SRC/PI3K/AKT signaling. J Ethnopharmacol. 2025;337(Pt 2):118898. doi: 10.1016/j.jep.2024.118898.
32. Wang L, Li J, Di LJ. Glycogen synthesis and beyond, a comprehensive review of GSK3 as a key regulator of metabolic pathways and a therapeutic target for treating metabolic diseases. Med Res Rev. 2022;42(2):946-82. doi: 10.1002/med.21867.
33. Muratsu J, Iwabayashi M, Sanada F, Taniyama Y, Otsu R, Rakugi H, et al. Hepatocyte growth factor prevented high-fat diet-induced obesity and improved insulin resistance in mice. Sci Rep. 2017;7(1):130. doi: 10.1038/s41598-017-00199-4.